

# An electrically tunable optical zoom system using two composite liquid crystal lenses with a large zoom ratio

Yi-Hsin Lin,\* Ming-Syuan Chen, and Hung-Chun Lin

Department of Photonics, National Chiao Tung University,  
1001 Ta Hsueh Rd., Hsinchu 30010, Taiwan

\*yilin@mail.nctu.edu.tw

<http://www.cc.nctu.edu.tw/~yilin>

**Abstract:** An electrically tunable-focusing optical zoom system using two composite LC lenses with a large zoom ratio is demonstrated. The optical principle is investigated. To enhance the electrically tunable focusing range of the negative lens power of the LC lens for a large zoom ratio, we adopted two composite LC lenses. Each composite LC lens consists of a sub-LC lens and a planar polymeric lens. The zoom ratio of the optical zooming system reaches  $\sim 7.9:1$  and the object can be zoomed in or zoomed out continuously at the objective distance of infinity to 10 cm. The potential applications are cell phones, cameras, telescope and pico projectors.

©2011 Optical Society of America

OCIS codes: (230.3720) Liquid-crystal devices; (230.2090) Electro-optical devices.

---

## References and links

1. R. Peng, J. Chen, and S. Zhuang, "Electrowetting-actuated zoom lens with spherical-interface liquid lenses," *J. Opt. Soc. Am. A* **25**(11), 2644–2650 (2008).
2. D. Y. Zhang, N. Justus, and Y. H. Lo, "Fluidic adaptive zoom lens with high zoom ratio and widely tunable field of view," *Opt. Commun.* **249**(1-3), 175–182 (2005).
3. K. Seidl, J. Knobbe, and H. Gröger, "Design of an all-reflective unobscured optical-power zoom objective," *Appl. Opt.* **48**(21), 4097–4107 (2009).
4. D. V. Wick, "Active optical zoom system," U.S. patent 6,977,777 (2004)
5. D. V. Wick, T. Martinez, D. M. Payne, W. C. Sweatt, and S. R. Restaino, "Active optical zoom system," *Proc. SPIE* **5798**, 151–157 (2005).
6. B. E. Bagwell, D. V. Wick, R. Batchko, J. D. Mansell, T. Martinez, S. Serati, G. Sharp, and J. Schwiegerling, "Liquid crystal based active optics," *Proc. SPIE* **6289**, 628908, 628908-12 (2006).
7. T. Martinez, D. V. Wick, D. M. Payne, J. T. Baker, and S. R. Restaino, "Non-mechanical zoom system," *Proc. SPIE* **5234**, 375–378 (2004).
8. E. C. Tam, "Smart electro-optical zoom lens," *Opt. Lett.* **17**(5), 369–371 (1992).
9. B. Wang, M. Ye, and S. Sato, "Liquid crystal lens with focal length variable from negative to positive values," *IEEE Photon. Technol. Lett.* **18**(1), 79–81 (2006).
10. S. Sato, "Liquid-crystal lens-cells with variable focal length," *Jpn. J. Appl. Phys.* **18**(9), 1679–1684 (1979).
11. M. Ye, B. Wang, and S. Sato, "Liquid-crystal lens with a focal length that is variable in a wide range," *Appl. Opt.* **43**(35), 6407–6412 (2004).
12. A. F. Naumov, M. Y. Loktev, I. R. Guralnik, and G. Vdovin, "Liquid-crystal adaptive lenses with modal control," *Opt. Lett.* **23**(13), 992–994 (1998).
13. H. W. Ren, Y. H. Fan, S. Gauza, and S. T. Wu, "Tunable-focus flat liquid crystal spherical lens," *Appl. Phys. Lett.* **84**(23), 4789–4791 (2004).
14. M. Ye, M. Noguchi, B. Wang, and S. Sato, "Zoom lens system without moving elements realized using liquid crystal lenses," *Electron. Lett.* **45**(12), 646 (2009).
15. P. Valley, M. Reza Dodge, J. Schwiegerling, G. Peyman, and N. Peyghambarian, "Nonmechanical bifocal zoom telescope," *Opt. Lett.* **35**(15), 2582–2584 (2010).
16. H. C. Lin, and Y. H. Lin, "A fast response and large electrically tunable-focusing imaging system based on switching of two modes of a liquid crystal lens," *Appl. Phys. Lett.* **97**(6), 063505 (2010).
17. H. C. Lin, and Y. H. Lin, "An electrically tunable focusing pico-projector adopting a liquid crystal lens," *Jpn. J. Appl. Phys.* **49**(10), 102502 (2010).
18. W. J. Smith, *Modern Optical Engineering*, 4th Ed. (McGraw-Hill Inc. New York, 2008)
19. Y. H. Lin, H. Ren, S. Gauza, Y. H. Wu, and S. T. Wu, "Single-substrate IPS-LCD using an anisotropic polymer film," *Proc. SPIE* **5936**, 593600, 593600-7 (2005).

20. Y. H. Lin, H. Ren, S. Gauza, Y. H. Wu, Y. Zhao, J. Fang, and S. T. Wu, "IPS-LCD using a glass substrate and an anisotropic polymer film," *J. Display Technol.* **2**(1), 21–25 (2006).
  21. Y. Choi, H. R. Kim, K. H. Lee, Y. M. Lee, and J. H. Kim, "A liquid crystalline polymer microlens array with tunable focal intensity by the polarization control of a liquid crystal layer," *Appl. Phys. Lett.* **91**(22), 221113 (2007).
- 

## 1. Introduction

An electrically tunable-focusing optical zoom system is important in many applications, such as cell phones, cameras, pico projectors and the night vision of hand-carried weapons [1–3]. A conventional optical zoom system consisting of many solid lenses, a mechanically controlled motor, and an image sensor is bulky and heavy. To realize an electrically tunable-focusing optical zoom system, several active-optical elements can be adopted, such as liquid lenses [1–2], deformable mirrors [3], and liquid crystal (LC) lenses [4–8]. The features of LC lenses are low cost, light weight, and no mechanical moving part. The main mechanism of electrically tunable focal length of LC lenses results from the gradient distribution of refractive indices owing to the orientations of LC directors [9–13]. In 1992, Tam did a theoretical analysis of electro-optical zoom lenses based on two spatial light modulators and two solid lenses, but did not show the experimental results [8]. In 2009, Ye et. al. realized a zoom lens system based on two LC lenses and a solid lens. However, the zoom ratio is only 1.5:1 because the electrically tunable focusing range of the negative lens power of the LC lens is not large enough. In addition, the location of an object and the size of the system are also limited by the solid lens [14]. In 2010, Valley et. al. proposed a nonmechanical bifocal zoom telescope based on two LC diffractive lenses within Fresnel zone electrodes [15]. The zoom ratio can reach ~4:1 but the image only has two discrete optical magnifications because the focal lengths of the LC diffractive lenses are not continuous switchable. Moreover, the Valley's zoom system can only apply to the object distance of infinity, the distance between two LC diffractive lenses is long (~50 cm) and the design of electrodes is complicated [15]. It is urgent to realize an electrically tunable-focusing optical zoom system based on LC lenses with a large zoom ratio, a small size of the system and a continuous tunable objective distance.

In this paper, we demonstrate a compact electrically tunable-focusing optical zoom system using two composite LC lenses with a large zoom ratio. We investigate the optical principle in the system first. In order to obtain a large zoom ratio, the electrically tunable focusing range of the negative lens power of the LC lens with two mode switching needs to be enhanced. A composite LC lens consisting of a sub-LC lens and a planar polymeric lens is adopted in the system. The zoom ratio of the optical zoom system reaches up to ~7.9:1 and the object can be zoomed in or zoomed out continuously at the objective distance of infinity to 10 cm. The experimental results agree with the theoretical results. The potential applications are cell phones, cameras, telescopes and pico projectors [16, 17].

## 2. Operating principles and sample preparation

The structure of the designed optical zoom system consisting of a target (or an object), a LC object lens, a LC eyepiece lens, and a camera system made up of a solid lens and an image sensor, as depicted in Fig. 1(a). The focal length of the LC object lens is  $f_o$ , and the focal length of the LC eyepiece lens is  $f_e$ . The distance between the target and the LC object lens is  $p$ , the distance between two LC lenses is  $d$ , and the distance between the LC eyepiece lens and the lens is  $q$ . Because the image sensor is located at the focal plane of the lens with a focal length of  $f_L$ , the light is incident on the lens should be collimated, so that the incident light can be collected into the image sensor.

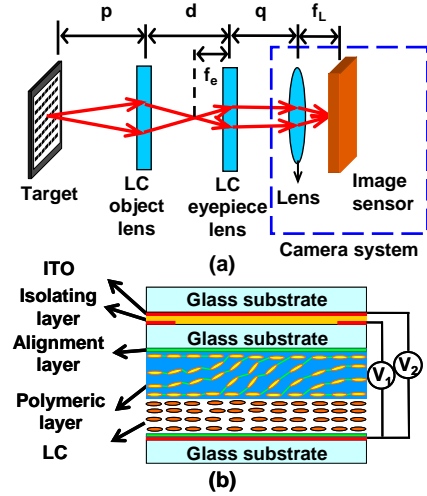


Fig. 1. (a) The structure of the zoom system and (b) the structure of the composite liquid crystal lenses for the LC object lens and the LC eyepiece lens in (a).

In order to obtain a collimated light right after the LC eyepiece lens, the relation among  $f_e$ ,  $f_o$ ,  $p$ , and  $d$  should be [18]:

$$\frac{1}{p} + \frac{1}{d - f_e} = \frac{1}{f_o}. \quad (1)$$

Equation (1) is then rearranged as:

$$f_e + \frac{f_o \times p}{p - f_o} = d. \quad (2)$$

From Eq. (2), the magnification ( $M$ ) of the optical zoom system in Fig. 1(a) can be written as:

$$M = \frac{f_o \times p}{(f_o - p) \times f_e}. \quad (3)$$

When  $p$  is near infinity,  $M$  equals to  $|f_o / f_e|$ . That means the optical zoom system is a telescopic system since two LC lenses are afocal (i.e.  $f_o + f_e = d$ ). We assume that magnification is positive (i.e. the erect image) and the LC lens could be switched as a positive or a negative lens. In the experiment, the minimum focal length of the positive LC lens is usually shorter than minimum absolute value of focal length of the negative LC lens under two mode switching of a LC lens. From Eq. (2) and Eq. (3), when we adjust  $f_o$  as a negative lens with a minimum absolute value of focal length (i.e.  $|f_{\min} < 0|$ ), the system has a minimum magnification ( $M_{\min}$ ):

$$M_{\min} = \frac{f_{\min} \times p}{f_{\min} \times p + f_{\min} \times d - d \times p}. \quad (4)$$

When  $f_e$  equals to  $f_{\min}$ , the system has a maximum magnification ( $M_{\max}$ ):

$$M_{\max} = \frac{f_{\min} - d}{f_{\min}}. \quad (5)$$

$M_{\max}$  and  $M_{\min}$  also limit the range of the magnification of the optical zooming system. The zoom ratio (ZR) of two LC lenses can be defined as the ratio of  $M_{\max}$  to  $M_{\min}$ . From Eq. (4) and Eq. (5), the ZR turns out:

$$ZR = \left(\frac{d}{f_{\min}} - 1 - \frac{d}{p}\right) \times \left(\frac{d}{f_{\min}} - 1\right). \quad (6)$$

From Eq. (6), the zoom ratio of the system is related to three parameters:  $d$ ,  $p$ , and  $|f_{\min}|$ . The system requires a smaller  $|f_{\min}|$  (or large  $f_{\min}$ ) in order to obtain a larger zoom ratio. In the previous published literatures, the zooming ratio is small (1.5:1) in the imaging system based on LC lenses because of the  $|f_{\min}|$  of LC lenses is large (i. e.  $f_{\min} < -10$  cm) [14]. Increasing  $d$  can increase the zoom ratio; however, the system would be too bulky. To obtain a compact system with a large zoom ratio, we developed a composite LC lens in Fig. 1(b) consisting of a sub-LC lens and a built-in planar polymeric lens in order to achieve a two mode switching of the composite LC lens, positive and negative lens. In addition, the minimum absolute value of focal length ( $|f_{\min}|$ ) of the composite LC lens is small.

The structure of the composite LC lens for the LC object lens and the LC eyepiece lens in Fig. 1(a) is depicted in Fig. 1(b). The composite LC lens consists of three Indium-Tin Oxide (ITO) glass substrates with thickness of 0.7 mm, an isolating layer (NOA 81, Norland Optical Adhesive) with thickness of 35  $\mu\text{m}$ , mechanically buffered alignment layers (Polyvinylalcohol or PVA), a polymeric layer with thickness of 35  $\mu\text{m}$ , and a LC layer with thickness of 50  $\mu\text{m}$ . The ITO layer in the middle of glass substrate was etched with a hole-pattern within a diameter of 1.28 mm. The fabrication process of the composite LC lens is also illustrated in Fig. 2(a), (b), (c), and (d). In Fig. 2(a), we first filled NOA 81 between two ITO glass substrates and exposed the UV light ( $\sim 1.25$  mW/cm<sup>2</sup>) for 20 min. The ITO layer in one of the glass substrate was etched with a hole-pattern within a diameter of 1.28 mm. Then we sandwiched the mixture between the structure in Fig. 2(a) and one ITO glass substrate which were coated with mechanically buffed PVA, as shown in Fig. 2(b). The filled mixture consisting of nematic LC, (MLC 2070, Merck,  $\Delta n = 0.26$  for  $\lambda = 589.3$  nm at 20°C), reactive mesogen (RM 82, Merck), and photoinitiator (IRG-184, Merck) at 30: 69: 1 wt% ratios. The cell was then applied 80 V<sub>rms</sub> ( $f = 1$  kHz) in order to generate a lens-like phase profile and exposed the UV light ( $\sim 1.25$  mW/cm<sup>2</sup>) for 40 min to freeze the phase profile by photopolymerization. After photopolymerization, we peeled off one of the substrates by a thermal releasing process, as depicted in Fig. 2(c). Then we sandwiched nematic LC mixture MLC-2070 between the polymeric layer and another ITO substrate coated with mechanically buffered PVA, as shown in Fig. 2(d). The polymeric layer has a fixed focal length ( $f_p$ )  $\sim -19$  cm because of the lens-like distribution of refractive indices generated by the voltage-curing process. The LC directors in the LC layer aligned by the polymeric layer and PVA were aligned homogeneously with pretilt angle  $\sim 2$  degree [19–21]. The composite LC lens was operated by two voltages, (i.e.  $V_1$  and  $V_2$  in Fig. 1(b)). The focal length of the composite LC ( $f_c(V_1, V_2)$ ) can be expressed as:

$$\frac{1}{f_c(V_1, V_2)} = \frac{1}{f_{LC}(V_1, V_2)} + \frac{1}{f_p}, \quad (7)$$

In Eq. (7),  $f_{LC}(V_1, V_2)$  is the voltage-dependent focal length of sub-LC lens contributed from the LC layer in Fig. 1(b). The  $f_{LC}(V_1, V_2)$  depending on the wavelength of light ( $\lambda$ ), aperture size ( $w$ ), and phase difference ( $\Delta\delta$ ) can be written as Eq. (8) [16,17]:

$$f_{LC}(V_1, V_2) = \frac{\pi \times w^2}{4 \times \lambda \times \Delta\delta(V_1, V_2)}. \quad (8)$$

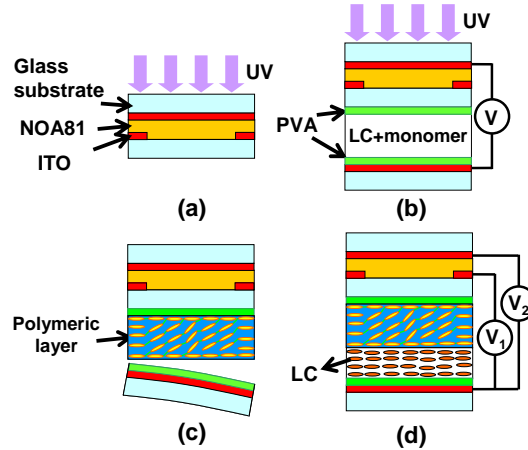


Fig. 2. Fabrication process of the composite LC lens. (a) Polymerize the isolating layer (b) polymerize the polymeric layer with a curing voltage of  $80 V_{\text{rms}}$ , (c) peel off the bottom substrate, and (d) sandwich the LC between (c) and another glass substrate.

### 3. Experimental results and discussion

To observe the phase profile of two composite LC lenses, we observed the image of the composite LC lenses at different voltages under crossed polarizers. Figure 3(a) shows the images of the composite LC lens. The rubbing direction of the composite LC lens was 45 degree with respect to one of the polarizers. In Fig. 3(a), the left one is the phase profile for the positive lens, and the right one is the phase profile for the negative lens. The number of concentric rings of Fig. 3(a) is proportional to the phase profile of the composite LC lens. We can convert the phase profile to the focal length according to the relation:  $f = D^2/8\lambda N$ , where  $D$  is the aperture size,  $\lambda$  is the wavelength,  $N$  is the number of rings of the phase profile. The lens powers, the inverse of focal length, of two composite LC lenses as a function of applied voltage are shown in Fig. 3(b). In Fig. 3(b), when  $V_1 > V_2$ , the LC layer acts as a positive lens that is because the tilt angles of LC directors of the LC layers in the center of the hole-electrode are smaller than those near the edge of the hole-electrode. Because of the polymeric layer with lens power  $\sim -5.3 \text{ m}^{-1}$ , the composite LC lens is a positive lens with the switchable lens power from  $21.8 \text{ m}^{-1}$  to  $0 \text{ m}^{-1}$  when  $0 < V_2 < 38 V_{\text{rms}}$  at  $V_1 = 80 V_{\text{rms}}$  and the composite LC lens is a negative lens with the switchable lens power from  $0$  to  $-5.3 \text{ m}^{-1}$  when  $V_2 > 38 V_{\text{rms}}$  at  $V_1 = 80 V_{\text{rms}}$ . At  $V_1 = 80 V_{\text{rms}}$  and at  $V_2 = 38 V_{\text{rms}}$ , the lens power of LC layer equals to the lens power of polymeric layer. As a result, the lens power of the composite LC lens is zero. When  $V_1 < V_2$ , the LC layer acts as a negative lens that is because the tilt angles of LC directors of the LC layers in the center of the hole-electrode are larger than those near the edge of the hole-electrode. At  $V_1 < 40 V_{\text{rms}}$  and  $V_2 = 40 V_{\text{rms}}$ , the composite LC lens is a negative lens with switchable lens power from  $-13.5 \text{ m}^{-1}$  to  $-5.3 \text{ m}^{-1}$  since both of the LC layer and the polymer layer are negative lenses. From Fig. 2(b), the  $f_{\text{min}}$  is around  $-7.4 \text{ cm}$  (i.e. lens power is  $-13.5 \text{ m}^{-1}$ .) The measured response time, including the rise time and the decay time, is around 4 sec when we switched the voltages between  $(V_1, V_2) = (80 V_{\text{rms}}, 80 V_{\text{rms}})$  and  $(V_1, V_2) = (80 V_{\text{rms}}, 0 V_{\text{rms}})$ . (The data are not shown here.)

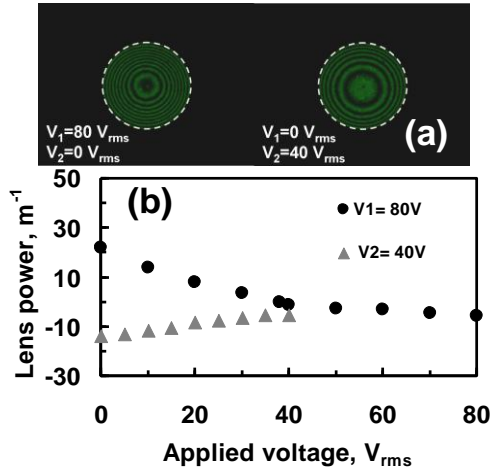


Fig. 3. (a) The phase profiles of the LC lens at different voltages. (b) The lens power of the composite LC lens as a function of applied voltage  $V_1$  when  $V_2$  was  $40 \text{ V}_{\text{rms}}$  (gray triangles) and the lens power of the composite LC lens as a function of applied voltage  $V_2$  when  $V_1$  was  $80 \text{ V}_{\text{rms}}$  (black dots).  $\lambda = 532 \text{ nm}$ .

To measure the zoom ratio of the system in Fig. 1(a), we attached a polarizer on the LC object lens whose transmissive axis is parallel to the rubbing direction. In Fig. 1(a),  $d$  was set as  $10 \text{ cm}$ , and  $q$  was  $1 \text{ cm}$ . We also placed a target with black squares with the area of  $0.55 \text{ mm} \times 0.55 \text{ mm}$  at  $p = 10, 20, 30, 50, 100 \text{ cm}$  and then adjusted voltages of two composite LC lenses to obtain the images with different magnifications ( $M$ ). By measuring the size change of the central square of the image, we can measure the magnification. The captured images for  $p = 10 \text{ cm}$  at  $M=1$ ,  $M_{\text{min}}$  and  $M_{\text{max}}$  are shown in Fig. 4 (a), (b), and (c).  $M_{\text{max}}$  and  $M_{\text{min}}$  are  $2.3$  and  $0.29$ , respectively. At  $p = 10 \text{ cm}$ , the image of the target can be magnified continuously from  $2.3 \times$  to  $0.29 \times$  depending on the voltage-dependent focal lengths of the composite LC lenses. The zooming ratio at  $p=10 \text{ cm}$ , the ratio of  $M_{\text{max}}$  to  $M_{\text{min}}$ , then equals to  $7.9:1$ .

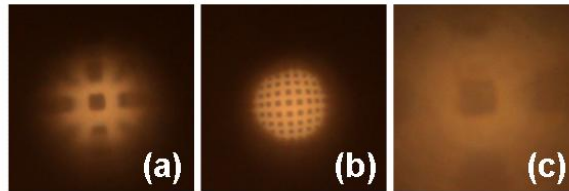


Fig. 4. Image performance of the zooming system when the target is at  $p$  of  $10 \text{ cm}$ . (a) Magnification ( $M$ )= $1$ ,  $f_o=10 \text{ cm}$  and  $f_e=\infty$ . (b)  $M=0.29$ ,  $f_o=-7.4 \text{ cm}$  and  $f_e=14.3 \text{ cm}$  (c)  $M=2.3$ ,  $f_o=6.4 \text{ cm}$  and  $f_e=-7.4 \text{ cm}$ . The zooming ratio is  $7.9:1$ .

The magnification as a function of  $p$  which is the distance between the target and the LC eyepiece lens is shown in Fig. 5. The maximum magnification (black dots in Fig. 5) remains similar around  $2.32$  as  $p$  increases. The minimum magnification (blue triangles in Fig. 5) increases from  $0.290$  to  $0.410$  as  $p$  increases. In Fig. 5, the target at different location can be zoomed in or zoomed out by switching the focal length of two composite LC lenses. After putting the experimental results:  $f_{\text{min}}=-7.4 \text{ cm}$  and  $d=10 \text{ cm}$  to Eq. (5), the theoretical maximum magnification independent of  $p$  is around  $2.35$  which is closed to the experimental result ( $\sim 2.32$ ). From Eq. (4), the minimum magnification increases from  $0.298$  to  $0.406$  with the increase of  $p$  which is also closed to the experimental results. From Fig. 5, we can obtain the zoom ratio as a function of  $p$  as shown in Fig. 6 (blue dots). The zoom ratio decreases from  $7.93:1$  to  $5.56:1$  when  $p$  increases from  $10 \text{ cm}$  to  $100 \text{ cm}$ . According to Eq. (6), the theoretical

zoom ratio as a function of  $p$  is also plotted in Fig. 5 (gray triangles). The experimental and theoretical results agree well. The zoom ratio is near 5.65 at  $p=200$  cm. Unlike the conventional optical zoom system based on mechanically moving solid lenses, the zoom ratio in our zooming system decreases with  $p$ , not a constant. In the conventional zoom system, the focusing lens and the zoom lens module are separated. However, in our zoom system, the LC object lens is in charge of focusing and zooming at the same time. Therefore, the zoom ratio is dependent on the location of the target.

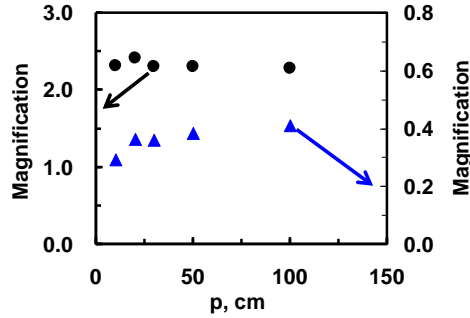


Fig. 5. The measured magnification as a function of the distance between target and the LC eyepiece lens (or  $p$ ). The black dots indicate the maximum magnification and the blue triangles indicate the minimum magnification.

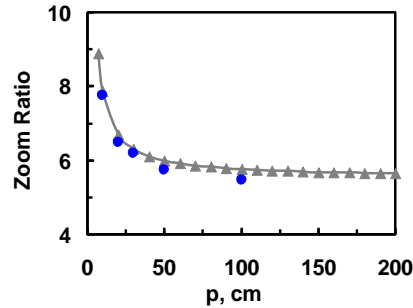


Fig. 6. The zoom ratio as a function of the distance between target and the LC eyepiece lens (or  $p$ ). The blue dots indicate the experimental results and the gray triangles indicate the simulation results.

To further enlarge the zoom ratio while maintaining small system size (i.e. small  $d$  in Fig. 1(a)), we can increase  $M_{\max}$  or decrease  $M_{\min}$ . To increase  $M_{\max}$  and decrease  $M_{\min}$ ,  $|f_{\min}|$  should be small. To obtain a composite LC lens with a small  $|f_{\min}|$ , we can further increase the negative focal length of the polymeric lens or increase the negative focal length of the sub-LC lens. To increase the negative focal length of the polymeric lens, we can increase the thickness of the polymeric layer or improve the distribution of refractive indices of the polymeric lens. The tradeoff is that the scattering increases with the thickness of the polymeric layer. To increase the negative focal length of the sub-LC lens, the phase difference inside the LC layer should be large. The phase difference can be enlarged by improving the birefringence of liquid crystal materials and enlarging the cell gap. However, the response time is also slow with a large cell gap of the sub-LC lens.

The image quality of a single LC lens should be good according to the phase profiles in Fig. 3(a) [17]. However, the zoomed images in Fig. 4 are poor due to the vignetting and distortion which are common aberrations in a zoom system [18]. The vignetting results from the small aperture size of two LC lenses ( $\sim 1.28$  mm). Increasing the aperture size or placing a

proper stop can reduce the vignetting. The distortion of an image is defined as the different magnifications of an image due to the displacement of the image from the paraxial position. The distortion is severe especially when the image size is big and the zoom ratio is large. To reduce the distortion, we can design special lens modules to reduce such an aberration.

#### **4. Conclusion**

We have demonstrated an electrically tunable focusing optical zoom system using two composite LC lenses. Our optical zoom system is compact and has large zoom ratio. The zoom ratio depending on the location of object is up to  $\sim 7.9:1$ . The object can be zoomed continuously by changing the voltage of two composite LC lenses. The related optical principle is also discussed. To improve the light efficiency, polarizer-free LC lenses with large aperture size or extra image stabilization system should be developed. By optimizing the structure of the composite LC lenses, the image quality can be improved for applications. We believe this study opens a new window in realizing cell phones, cameras, telescopes and pico projectors.

#### **Acknowledgments**

The authors are indebted to Ms. Hsin-Ju Su for the technical assistance. This research was supported by the National Science Council (NSC) in Taiwan under the contract no. 98-2112-M-009-017-MY3.